

CHEMICAL EVOLUTION AND THE GALACTIC HABITABLE ZONE OF M31 (THE ANDROMEDA GALAXY)

Leticia Carigi,¹ Sofía Meneses-Goytia,^{1, 2} and Jorge García-Rojas^{3,4}

Draft version: August 22, 2012

RESUMEN

Calculamos la Zona de Habitabilidad Galáctica (ZHG) de M31 basándonos, principalmente, en la probabilidad de formación de planetas terrestres dependiente de la metalicidad (Z) del medio interestelar. La ZHG fue determinada a partir de un modelo de evolución química construido para reproducir un gradiente de metalicidad preciso en el disco galáctico: $[O/H](r) = -0.015 \pm 0.003 \text{ dex kpc}^{-1} \times r(\text{kpc}) + 0.44 \pm 0.04 \text{ dex}$. Este gradiente es el más probable en presencia de dispersión intrínseca en los datos observacionales. El modelo de evolución química predice una formación estelar más activa y una formación galáctica menos eficiente, comparada con las de la Vía Láctea. Suponiendo que los planetas tipo Tierra se forman bajo una ley de probabilidad que sigue la distribución de Z mostrada por las estrellas con planetas, entonces la ZHG más probable con vida simple se localiza entre 6 y 17 kpc en planetas con edades entre 1 y 4.5 Gigaños, mientras que la ZHG más probable con vida compleja sobreviviente a explosiones de supernovas se localiza entre 3 y 13 kpc en planetas con edades entre 4.5 y 6.5 Gigaños. Debido a que la historia de formación estelar de M31 ha sido más eficiente y que su ZHG es más amplia y vieja que en nuestra galaxia, el número de planetas que puede albergar vida en M31 podría ser mayor que en nuestra Galaxia.

ABSTRACT

We have computed the Galactic Habitable Zones (GHZs) of the Andromeda galaxy (M31) based mainly, but not exclusively, on the probability of terrestrial planet formation, which depends on the metallicity (Z) of the interstellar medium. The GHZ was therefore obtained from a chemical evolution model built to reproduce a precise metallicity gradient in the galactic disk, $[O/H](r) = -0.015 \pm 0.003 \text{ dex kpc}^{-1} \times r(\text{kpc}) + 0.44 \pm 0.04 \text{ dex}$. This gradient is the most probable when intrinsic scatter is present in the observational data. The chemical evolution model predicted a higher star formation history in both the halo and disk components of M31 and a less efficient inside-out galactic formation, compared to those of the Milky Way. If we assumed that Earth-like planets form with a probability law that follows the Z distribution shown by stars with detected planets, the most probable GHZ with basic life is located

¹Instituto de Astronomía, Universidad Nacional Autónoma de México. Apartado Postal 70-264, Ciudad Universitaria, México DF 04510, México.

²Kapteyn Instituut, Rijkuniversiteit Groningen. Landleven 12, 9747 AD, Groningen, Nederland.

³Instituto de Astrofísica de Canarias. E-38200. La Laguna, Tenerife, Spain.

⁴Departamento de Astrofísica, Universidad de La Laguna. E-38205. La Laguna, Spain.

between 6 and 17 kpc on planets with ages between 4.5 and 1 Gy, and the most probable GHZ with complex life that survived supernova explosions is located between 3 and 13 kpc on planets with ages between 6.5 and 4.5 Gy. Since the star formation history of M31 has been more efficient and its GHZ is wider and older compared to those of the Milky Way, the number of planets harboring life in M31 may be higher than that of our galaxy.

Key Words: Galactic habitability — Chemical evolution — Abundance gradients — Andromeda galaxy — M31

1. INTRODUCTION

The Galactic Habitable Zone (GHZ) is defined as the region with sufficient abundance of chemical elements to form planetary systems in which Earth-like planets could be found and might be capable of sustaining life (Gonzalez et al. 2001, Lineweaver 2001). An Earth-like planet is a rocky planet characterized in general terms by the presence of water and an atmosphere (Segura & Kaltenegger 2009).

GHZ research has focused mainly on our galaxy, the Milky Way (MW) (Gonzalez et al. 2001, Lineweaver et al. 2004, Prantzos 2008, Gowanlock et al. 2011). Gonzalez et al. were the first to propose the concept of a Galactic Habitable Zone, which is a ring located in the thin disk that migrates outwards with time. Lineweaver et al. (2004) later proposed that the Milky Way's GHZ is a ring located in the Galactic disk within a radius interval of 7 to 9 kpc from the center of the MW, and that the area of the ring increases with the age of the Galaxy. On the other hand, Prantzos concluded that the current GHZ is a wider ring that covers practically the entire MW disk. These studies confirmed that the Solar System is located within the GHZ since the Sun is found at 8 kpc from the center of the Galaxy. Nevertheless, a star with an Earth-like planet capable of sustaining life is more likely to be found in inner rings of the Galactic disk, between 2 and 4 kpc, owing to the high stellar surface density that presents the inner disk of our galaxy (Prantzos 2008, Gowanlock et al. 2011).

The GHZ has recently been computed for two elliptical galaxies (Suthar & McKay 2012). Imposing only metallicity restrictions for planet formation, these authors found that both elliptical galaxies could sustain broad GHZs.

Here, we extend MW studies to the disk of the most massive galaxy in the Local Group: the Andromeda galaxy (M31). M31 is a type SAb spiral galaxy, whose visible mass is 1. times larger than that of the MW, and M31 is at a distance of 783 ± 30 kpc (Holland 1998).

The GHZ depends mainly on the abundance of chemical elements heavier than He (metallicity, Z), since Z leads to planetary formation. Moreover, the GHZ also depends on the occurrence of supernovae (SNe), since SNe determine regions where planets can survive possible sterilization.

In this paper, we excluded the bulge of Andromeda from the GHZ, despite its having a high enough abundance of chemical elements to form planets

(Sarajedini & Jablonka 2005). The bulge does not provide a stable habitat for life due to its high supernovae rate, which could sterilize planets (Meneses-Goytia 2009), and the proximity of stars that can destabilize the orbits of the planets (Jiménez-Torres et al. 2011).

Throughout this paper the terms "evolved life" and "complex life" are synonymous. These terms refer to a type of life similar to that of the human beings, since they are able to develop advanced technologies.

In this study, we present a chemical evolution model (CEM) for the halo and disk components that predicts the temporal behavior of the space distribution of Z and supernova occurrence in M31, built on precise observational constraints (Sec. 2). Based on a set of biogenic, astrophysical, and geophysical restrictions, the CEM results lead to the determination of the GHZ (Sec. 3). We discuss the implication of the chemical evolution model and the GHZ condition on the location, size, and age of the Galactic Habitable Zone (Sec. 4). Finally, we present our conclusions of the present study (Sec. 5).

2. CHEMICAL EVOLUTION MODEL, CEM

Chemical evolution models study the changes, in space and time, of: a) the chemical abundances present in the interstellar medium (ISM), b) the gas mass, and c) the total baryonic mass of galaxies and intergalactic medium. These studies have a considerable number of free parameters and observational constraints allow us to estimate some of them. If the number of observational constraints is high and the observational data are precise, a more solid model can be proposed and therefore a better GHZ inferred. In consequence, before building the CEM, we collected and determined a reliable chemical data set.

2.1. *Observational constraints*

The present CEM was built to reproduce M31's three main observational constraints of the galactic disk: the radial distributions of the total baryonic mass, the gas mass, and the oxygen abundance. Since the data come from several authors, who have adopted different distances, the data used in this work were corrected according to our adopted distance of 783 kpc for M31.

2.1.1. *Radial distribution of the total mass surface density in the disk, $\Sigma_T(r)$*

The luminosity profile is produced by the stellar and ionized gaseous components of the galaxies. In evolved spiral galaxies, such as M31, the current luminosity is mostly due to the stellar component. Because the luminosity profiles of such galaxies follow an exponential behavior with respect to galactocentric distance (r), we associated that profile to the radial distribution of total mass surface density, $\Sigma_T(r) = \Sigma_0 \exp(-r/r_d)$ where $r_d = 5.5$ kpc (Renda et al. 2005). The value for Σ_0 is $548.2 \text{ M}_\odot \text{ pc}^{-2}$ and was obtained by the integration of $\Sigma_T(r)$ over the disk's surface in order to reproduce the total mass disk of M31, which is $7.2 \times 10^{10} \text{ M}_\odot$ (Widrow, Perrett & Suyu 2003).

2.1.2. Radial distribution of oxygen abundance, $[O/H](r)$

The data were taken from the compilation of M31's ionized hydrogen (HII) region spectra by Blair et al. (1982) and Galarza et al. (1999). From the total region sample, we rejected those with uncertain measurements of [OII], [OIII], and [NII] lines.⁵ Taking into account these prescriptions, the final number of HII regions of our sample is equal to 83. Once we selected our sample, we employed the R_{23} bi-evaluated method from Pagel et al. (1979), which links the intensity of strong [OII] and [OIII] emission lines with [O/H], to compute the abundances.

The disadvantage of this method is that it is double-valued with respect to metallicity. In fact, at low oxygen abundances ($[O/H] \leq -0.66$) the R_{23} index decreases with the abundance, while for high oxygen abundances ($[O/H] \geq -0.41$) the metals cooling efficiency makes R_{23} drop with rising abundance. In order to break the R_{23} method's degeneracy, we used [NII]/[OII] line ratios, which are not sensitive to the ionization parameter and are a strong function of O/H above $\log([NII]/[OII]) \geq 1.2$ (Kewley & Dopita, 2002).

To obtain an estimation of the uncertainties in the abundances, we have propagated the error in the line fluxes and added quadratically the accuracy of each method, which is between ± 0.1 - 0.2 dex. It is worth mentioning that the oxygen abundances derived in this study correspond to the composition of the ionized gas phase of the interstellar medium, without taking into account oxygen depletion in dust grains.

In this study, we express the chemical abundances as a function of the galactocentric distance (r), related to the Sun as: $[O/H](r) = \log(O/H)(r) - \log(O/H)_{\odot}$, where (O/H) represents the ratio of the abundance by number of oxygen and of hydrogen, and $(O/H)_{\odot}$ is this ratio in the Sun, which has a value of -3.34 dex (Grevesse, Asplund & Sauval 2007). Moreover, the radial abundance gradient is expressed by the slope and y-intercept value of a linear relationship that fits the trend of empirical abundances as a function of r .

The Galactocentric distances of the objects have been derived taking into account the Galactocentric distances derived by Blair et al. (1982) and Galarza et al. (1999), recomputed for an inclination angle, $i = 77^{\circ}$, and adopting the distance to M31 from Holland (1998): 783 ± 30 kpc.

In Figure 1, we compile the radial [O/H] gradients obtained from the different empirical and theoretical calibrations. It is clear that all the theoretical methods give very similar results in contrast to the empirical methods, which have much lower y-intercept values even though they keep similar slopes.

Additionally, we tested the effect of the presence of intrinsic scatter in the data in a similar manner to Rosolowsky & Simon's (2008) method for the gradient of M33 (the third spiral galaxy of the Local Group). Following these authors' procedure, we applied the method of Akritas & Bershady (1996) to compute the gradients in the presence of an intrinsic scatter. We constructed histograms for each calibration taking into account samples of ten HII regions

⁵The notation [XI] implies the atom X in neutral form, [XII] indicates X^{+} , [XIII] is X^{2+} , etc

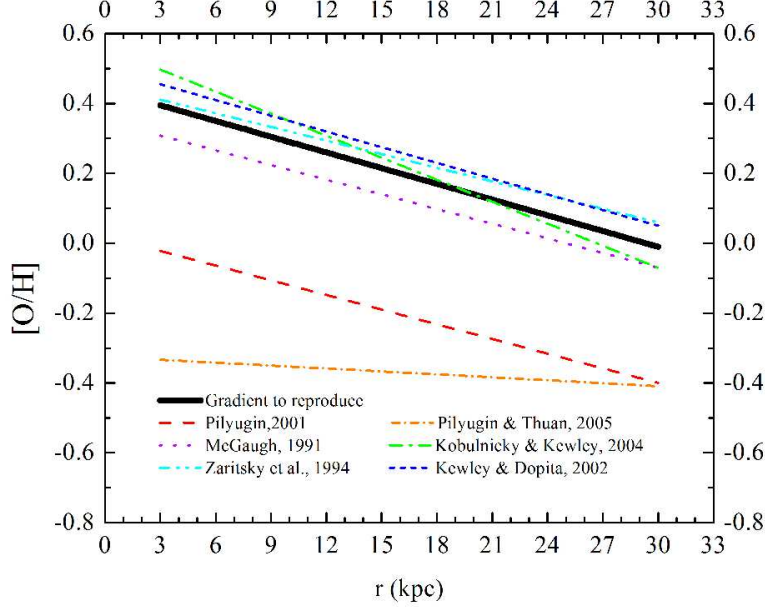


Fig. 1. Gradients obtained using different calibration methods. Empirical methods: Pilyugin (2001) and Pilyugin & Thuan (2005). Theoretical methods: McGaugh (1991), Kewley & Dopita (2002), Kobulnicky & Kewley (2004), and Zaritsky et al. (1994). The most probable gradient among the theoretical methods, applying the method of Akritas & Bershadsky (1996) (see section 2.1.3), is indicated by the broad line. That gradient is the one to be reproduced by the chemical evolution model. Note that the theoretical methods give very similar results.

drawn randomly and we obtained the distributions shown in Figure 2. The final adopted gradient is the weighted average of the four theoretical calibrations we have considered. Hence, the adopted slope is -0.015 ± 0.003 dex kpc^{-1} and the y-intercept value of $[\text{O}/\text{H}]$ at the center of M31 is 0.44 ± 0.04 dex. Finally, we adopted two gradients with which to work: at first, the gradient obtained as the most probable value using the method of Akritas & Bershadsky (1996) ($[\text{O}/\text{H}](r) = -0.015 \pm 0.003$ dex $\text{kpc}^{-1} \times r(\text{kpc}) + 0.44 \pm 0.04$ dex), which we considered to be representative of the gradients obtained by using photoionization model calibrations. On the other hand, we tried to explore the chemical evolution of M31 by adopting the gradient given by Pilyugin's (2001) empirical calibration, $[\text{O}/\text{H}](r) = -0.014 \pm 0.004$ dex $\text{kpc}^{-1} \times r(\text{kpc}) + 0.02 \pm 0.05$ dex), a gradient with similar slope but with a y-intercept value 0.42 dex lower compared to the most probable gradient obtained from theoretical calibrations. We also tested the gradient given by Pilyugin & Thuan's (2005) empirical calibration, which gives a slope 0.006 dex kpc^{-1} flatter than all the other calibrations with an intermediate y-intercept value (see section 4.1 for a more detailed discussion).

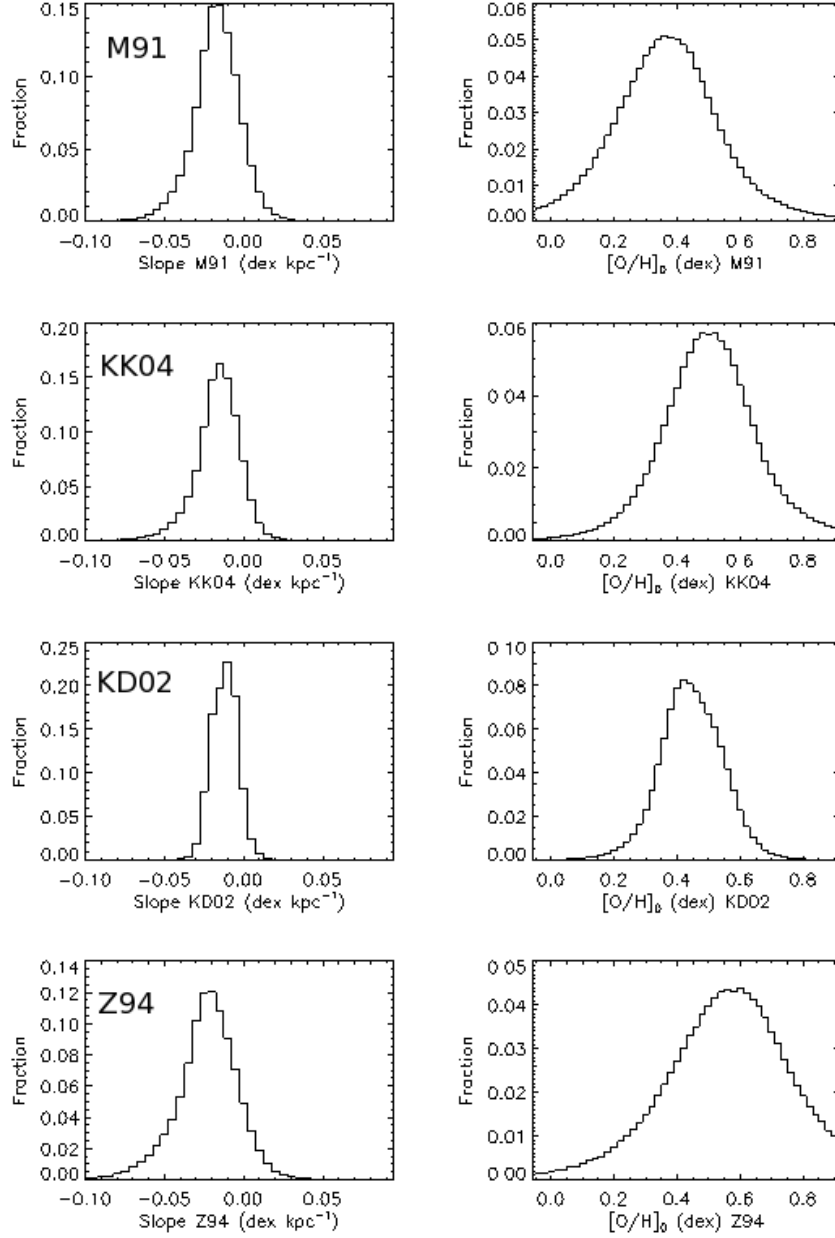


Fig. 2. Distribution of the slope (left) and y-intercept (right) of the O/H gradients obtained from the four theoretical calibrations considered in this work: McGaugh (1991) (M91), Kobulnicky & Kewley (2004) (KK04), Kewley & Dopita (2002) (KD02) and Zaritsky et al. (1994) (Z94). The distributions are for samples of ten HII regions drawn randomly from the total sample (see text). See figure 5 of Rosolowsky & Simon (2008) for a similar diagram in M33.

2.1.3. Radial distribution of the gas mass surface density, $\Sigma_{gas}(r)$

$\Sigma_{gas}(r)$ represents all gaseous stages which contain hydrogen, helium, and the rest of the chemical elements, i.e. $\Sigma_{gas}(r) = \Sigma_H + \Sigma_{He} + \Sigma_Z$.

E. M. Berkhuijsen (2008, private communication), based on Nieten et al. (2006), kindly provided us with the updated atomic and molecular surface density of hydrogen for the northern and southern halves of the disk of M31. We averaged out these data to obtain Σ_H . Taking into account the He and O enrichment by Carigi & Peimbert (2008) ($He = 0.25 + 3.3 \times O$, where He and O are abundances by mass), the $[O/H]$ gradient shown in the previous subsection, and scaling O and Z to solar values, we computed Σ_{He} and Σ_Z . As additional Σ_H data, we used the compilation of Renda et al. (2005), which was corrected following the previously described procedure.

In Figure 3a we show both sets of corrected data which we used as $\Sigma_{gas}(r)$ constraints on our chemical evolution model.

2.2. Model's assumptions

In the present article, we built a dual-infall model in an inside-out formation framework (i.e., the galaxy is formed more efficiently in the inner regions than at the periphery), similar to the model used by Renda et al. (2005), Hughes et al. (2008), and Carigi & Peimbert (2011) based on the following assumptions:

1. The halo and the disk are artificially projected onto a single disk component of negligible width with azimuthal symmetry; therefore, all functions depend only on the galactocentric distance (r) and time (t).
2. M31 was formed by a dual-infall, $d\Sigma_T(r, t)/dt$, of primordial material ($H = 0.75$ and $He = 0.25$, which are the abundances by mass of hydrogen and helium, respectively) given by the following expression:

$$d\Sigma_T(r, t)/dt = a_h(r)e^{-t/\tau_h} + a_d(r)e^{-(t-1\text{Gy})/\tau_d}.$$

The first term represents the halo formation during the first gigayear (Gy), $a_h(r)$ was obtained considering the halo's present-day total surface density profile as $6M_\odot\text{pc}^2/(1 + (r/8\text{kpc})^2)$ and $\tau_h = 0.1$ Gy according to Renda et al. (2005).

The second term represents the disk formation from 1 Gy until $t_g = 13$ Gy (current time), where $a_d(r)$ was obtained from $\Sigma_T(r)$ (see section 2.1.1), $\tau_d = 0.45$ (r/kpc) Gy, which represents the inside-out scenario and such a value was adopted to reproduce the $\Sigma_{gas}(r)$ along with $[O/H](r)$ (see sections 2.1.2 and 2.1.3).

3. The star formation rate (SFR) is the amount of gas which is transformed into stars and was parameterized as the Kennicutt–Schmidt law (Kennicutt, 1998), $\text{SFR}(r, t) = \nu \Sigma_{gas}^n(r, t)$, where ν is the efficiency of star formation and n is a number between 1 and 2. During the halo phase, we

chose $n = 1.0$ and we obtained $\nu = 0.50 \text{ Gy}^{-1}$ in order to reproduce the maximum average of metallicity shown by the halo stellar population, $\log(Z/Z_{\odot}) = -0.5 \text{ dex}$ (Koch et al. 2008) ($Z_{\odot} = 0.012$ from Grevesse, Asplund & Sauval, 2007). For the disk phase, we chose $n = 1.45$, a typical value for the disk of spiral galaxies (Fuchs, Jahreiß & Flynn 2009), and we obtained $\nu = 0.23 \text{ Gy}^{-1} (\text{M}_{\odot}/\text{pc}^2)^{-0.45}$ in order to reproduce $\Sigma_{gas}(r)$ along with $[\text{O}/\text{H}](r)$ restrictions at the present time.

4. The initial mass function (IMF) is the mass distribution of the stars formed. We considered the IMF of Kroupa et al. (1993), between a stellar mass interval of 0.1 to 80 M_{\odot} , since the chemical evolution models that assume this IMF successfully reproduce the chemical properties of the MW's halo-disk (Carigi et al. 2005).
5. We adopted the instantaneous recycle approximation, which assumes that stars whose initial mass is higher than 1 M_{\odot} die instantly after being created and the chemical elements they produce are ejected into the interstellar medium. This approximation is good for the elements produced mainly by massive stars, such as oxygen, since those stars have short lifetimes (10^{-3} to 10^{-2} Gy). The stellar mass fraction returned to the ISM by the stellar population and chemical yields are taken from Franco & Carigi (2008).
6. The loss of gas and stars from the galaxy to the intergalactic medium was not considered. All chemical evolution models of spiral galaxies reproduce the observational constraints without assuming material loss from the galactic disk (e.g. Carigi & Peimbert, 2011). Moreover, no substantial amount of gas surrounding either M31 or the MW has been observed.
7. We do not include radial flows of gas or stars.

2.3. Results of the Chemical Evolution Model

Based on the previously mentioned assumptions and the proper values of the free parameters chosen in order to reproduce $\Sigma_T(r, t_g)$, $\Sigma_{gas}(r, t_g)$ and the most probable $[\text{O}/\text{H}]$ gradient (see section 2.1) at the present time, we obtained the following results:

2.3.1. Radial distribution of the gas mass surface density, Σ_{gas}

Σ_{gas} was solved numerically for each radius at different times. With the halo and disk prescriptions shown in section 2.2, the predicted Σ_{gas} at the present time was found and depicted in Figure 3a along with the data. The maximum of the theoretical Σ_{gas} is shifted towards the inner radius compared to the observed values, but the agreement with the central and outer radius is quite good.

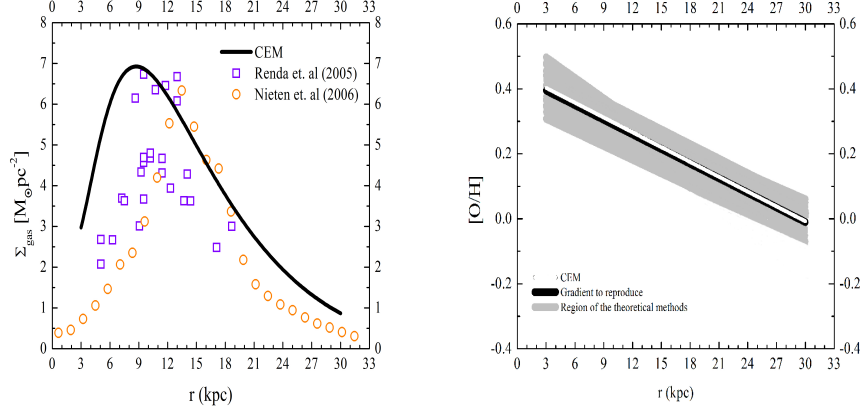


Fig. 3. Results of the chemical evolution model (CEM) at the present-time compared to the observational data. a) Radial distribution of the gas mass surface density (see section 2.1.3). b) [O/H] gradient. The white line is the predicted gradient; the black line represents the most probable gradient and the shaded area compiles the gradients obtained by the theoretical methods (see section 2.1.2).

We could improve the Σ_{gas} agreement for $r < 8$ kpc, but the slope of the chemical gradient (the most important constraint in this study) became steeper than the most probable one and it was not precise enough to reproduce the chemistry.

To improve the agreement of Σ_{gas} for $r < 8$ kpc it may be necessary to assume gas flows through the disk towards the galactic center, as an effect of the Galactic bar (Portinari & Chiosi 2000, Spitoni & Matteucci 2011), which is beyond the scope of this paper.

2.3.2. Chemical abundances

The CEM was built to mainly reproduce the O/H gradient determined in this study. That gradient is precise and allowed us to obtain a reliable chemical history for M31, where the GHZ will be supported.

In Figure 3b we present the [O/H] gradient predicted by the model at the present time (13 Gy) compared with the observational constraints for M31. The gradients obtained by the theoretical methods were enclosed in the shaded area of the figure, and the adopted gradient, $[O/H] = -0.015 \text{ dex kpc}^{-1} \times r \text{ (kpc)} + 0.44 \text{ dex}$, was also included in the figure as a broad white line. The gradient obtained from the CEM, $[O/H] = -0.015 \text{ dex kpc}^{-1} \times r \text{ (kpc)} + 0.45 \text{ dex}$, represented by a solid black line in the figure, is in perfect agreement with the observed value, ensuring the predicted metallicity history.

As previously described, oxygen is the most abundant elemental component of Z ; a chemical evolution model built to reproduce the [O/H] gradient therefore allows an adequate approximation of the evolution of the heavy elements, represented by Z .

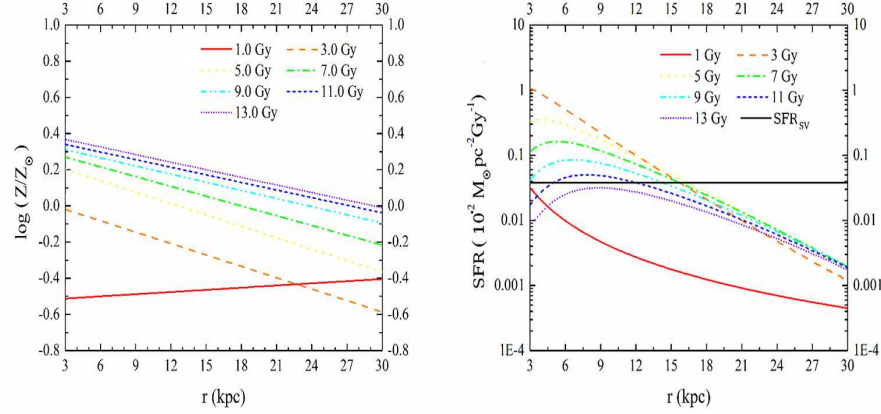


Fig. 4. Evolution of radial distributions at 1, 3, 5, 7, 9, 11, and 13 Gy. a) Metallicity relative to the solar value, $\log(Z/Z_{\odot})$ ($Z_{\odot} = 0.012$, Grevesse et al. 2007). b) Star formation rate, SFR. The horizontal line represents the average value of the SFR that the solar neighborhood has undergone during the Sun's lifetime. (Carigi & Peimbert 2008).

Since the GHZ depends mainly on metallicity, we are interested in the evolution of the metal radial distribution; hence, in Figure 4a we show the behavior of $\log(Z/Z_{\odot})$ with respect to galactocentric distances at different times. It is not surprising that the current gradient of $\log(Z/Z_{\odot})$, $\log(Z/Z_{\odot}) = -0.015 \text{ dex kpc}^{-1} \times r \text{ (kpc)} + 0.41 \text{ dex}$, is similar to the $[\text{O}/\text{H}]$ gradient obtained by the CEM, $[\text{O}/\text{H}] = -0.015 \text{ dex kpc}^{-1} \times r \text{ (kpc)} + 0.45 \text{ dex}$, confirming that oxygen is the most abundant heavy element and behaves as Z .

From Figure 4a, we notice that the gradient flattens from 3 to 13 Gy, due to the inside-out scenario: at the beginning of the evolution the infall was relevant in the central regions compared to the outer parts, producing higher Σ_{gas} and SFR, rapidly increasing the oxygen abundance in the inner regions; then the infall, and therefore the SFR, dropped, causing a lower increase in the oxygen abundance. In contrast, at the final stages of the evolution, the infall became important in the outer regions compared to the inner regions, thus Σ_{gas} increased and SFR became more efficient, producing a higher increase in the O abundance in outer regions and, consequently, the gradient became flatter.

The positive slope of the Z gradient at 1 Gy is quite remarkable. This opposite slope behavior is due to the enormous amount of primordial material, from the intergalactic medium, that fell into the inner parts at the beginning of the disk formation, causing gas dilution and a consequent decrease in the O/H values.

2.3.3. *Supernova rate*

As we have mentioned, the occurrence of supernovae (SNe) is important in the calculation of the GHZ because a high SN rate may destroy the atmosphere and life of a planet. From the star formation rate inferred by our chemical evolution model, we obtained the SN rate. It was computed according to $RSN(t) = N_{MS} \times SFR(t)$, where $N_{MS} = 0.05 M_{\odot}^{-1}$ is the number of type II supernova progenitors per M_{\odot} . We assumed that those progenitors are stars more massive than $8 M_{\odot}$ and therefore N_{MS} was calculated by integrating the initial mass function between 8 and $80 M_{\odot}$.

In Figure 4b, we show the star formation rate as a function of galactocentric distance for the same times shown in Figure 4a. In order to compare with the SFR that occurred in the solar neighborhood during the Sun's lifetime, we added the average value of the SFR in the solar neighborhood over the last 4.5 Gy. That average was obtained from the mean SFR at the solar radius during the last 4.5 Gy, $\langle SFR(8 \text{ kpc}) \rangle = \langle SFR_{SV} \rangle = 3.8 M_{\odot} \text{ Gy}^{-1} \text{ pc}^{-2}$ (see Fig. 2 by Carigi & Peimbert 2008). Consequently, the 4.5 Gy average SN rate of the solar neighborhood is $\langle RSN_{SV} \rangle = 0.2 \text{ Gy}^{-1} \text{ pc}^{-2}$.

3. GALACTIC HABITABLE ZONE

The Galactic Habitable Zone (GHZ), is defined as the region with sufficient abundance of chemical elements to form planetary systems in which Earth-like planets could be found and might be capable of sustaining life. Therefore, a minimum metallicity is needed for planetary formation, which would include the formation of a planet with Earth-like characteristics (Gonzalez et al. 2001, Lineweaver 2001), and a CEM provided the evolution of the heavy element distribution (see previous section).

3.1. *Characteristics and conditions for the GHZ*

In this context, it is important to bear in mind the properties and characteristics that an Earth-like planet and its environment need in order to be considered habitable or leading to habitability. In astrobiology, the chemical elements are classified according to the roles they play in the formation of an Earth-like planet and in the origin of life: the major biogenic elements are those that form amino acids and proteins (e.g. H, N, C, O, P, S), the geophysical elements are those that form the crust, mantle, and core (e.g. Si, Mg, Fe) (Hazen et al. 2002).

3.1.1. *Astrophysical conditions*

The conditions of the environment around an Earth-like planet are the following:

1. Planet formation: The metallicity in the medium where the planet may form (protoplanetary disk) must be such that it allows matter condensation and hence protoplanet formation (Lineweaver 2001). Therefore, Earth-like and Jupiter-like planets may be created. Whether the creation of Jupiter-like planets is beneficial or not is a debatable subject (Horner & Jones 2008, 2009). They may act as a shield against meteoritic impact (Fogg & Nelson 2007, Ward & Brownlee 2000), or might migrate towards the central star of the planetary system, thereby affecting the internal planets, or even destroying them (Lineweaver 2001, Lineweaver et al. 2004). On the other hand, the simulation by Raymond et al. (2006) predicts that Earth-like planets may form from surviving material outside the giant planet's orbit, often in the habitable zone and with low orbital eccentricities. Most ($\sim 90\%$) of the planet-harboring stars, detected by several research teams, show a wide range of stellar metallicity, $-0.35 \leq \log(Z/Z_{\odot}) \leq +0.35$, and the distribution peaks at $\log(Z/Z_{\odot}) \sim +0.20$ (See Figure 5). Data compilation taken from The Extrasolar Planets Encyclopaedia on July 2012, <http://exoplanet.eu/catalog.php>). Moreover, based on the same data source, the observed relation between stellar Z abundance and the planet mass presents a wide dispersion. Since that sample includes all types of planets—both Earth-like and Jupiter-like—the stellar Z –planet mass relation does not show a clear trend. Recently, Jenkins et al. (2012) have grown the population of low-mass planets around metal-rich stars, increasing the dispersion in the stellar Z –planet mass relation. Therefore we think that the $\log(Z/Z_{\odot})$ range represents the necessary Z to form planets that survive to planetary migrations. It should be mentioned that the stellar Z is associated with the planet Z since the planets were created from the same gaseous nebula of the star.

2. Survival from SNe: When a supernova explodes, it emits radiation capable of wiping out the atmosphere of a nearby planet and sterilizing the life that may lie on its surface (Lineweaver et al. 2004, Gowanlock et al. 2011). Since the Earth is the only known planet with life, we assumed it represents the survival pattern to SN explosions. We considered a planet to survive if the rate of SN (RSN) exploding, within a distance of 0.1 kpc, is the same or less than the time-average, during the last 4.5 Gy of SN rate in the solar neighborhood ($\langle RSN_{SV} \rangle$), where the Sun and its planets formed. That number is $\langle RSN_{SV} \rangle = 0.2 \text{ Gy}^{-1} \text{ pc}^{-2}$ (see section 2.3.3). We have analyzed two possibilities for the planet survival: i) the life on the planet will be annihilated forever when the instantaneous $RSN(t)$ is higher than $\langle RSN_{SV} \rangle$, and ii) the exoplanet will be sterilized when the average RSN , during the entire existence of the planet, is higher than $\langle RSN_{SV} \rangle$.

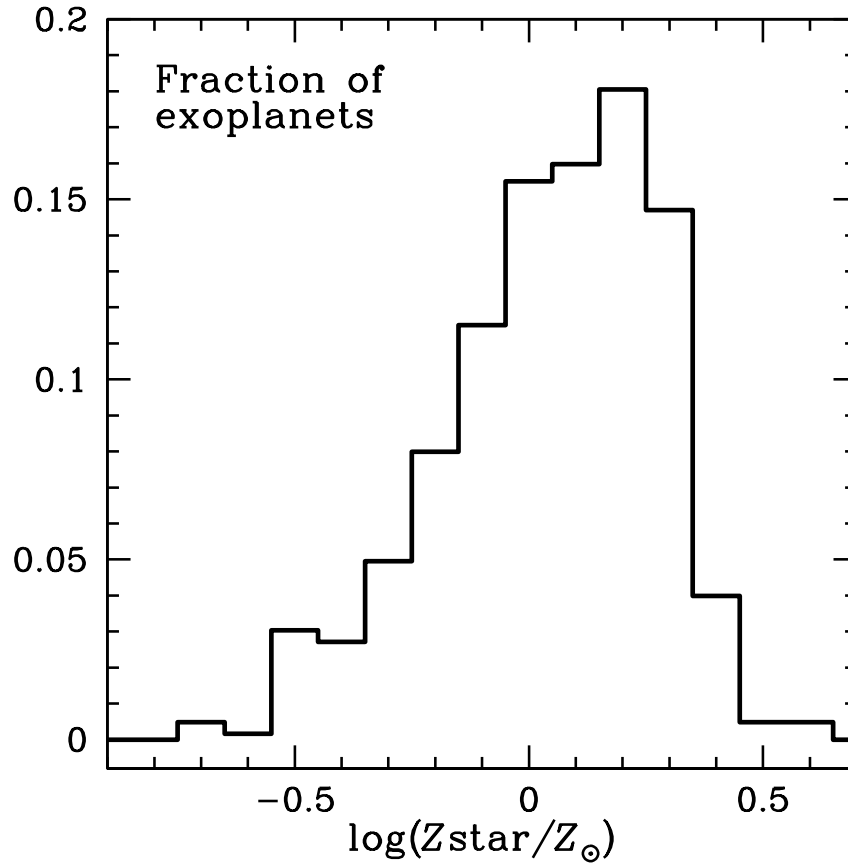


Fig. 5. The fraction of detected exoplanets as a function of the metallicity of the stars with exoplanets. Data compilation taken from The Extrasolar Planets Encyclopaedia on July 2012, <http://exoplanet.eu/catalog.php>.

3.1.2. Geophysical characteristics

An Earth-like planet is one that has enough biogenic and geophysical elements to sustain and allow the development of life as it is known on Earth (Sleep, Bird & Pope 2012, Bada 2004, Gomez-Caballero & Pantoja-Alor 2003, Hazen et al. 2002, Orgel 1998). In general terms, for a planet to be identified as an Earth-like planet, it has to satisfy the following conditions:

1. Tectonic plates: a crust formed mainly of Si constitutes the tectonic plates. These are necessary since life must have a site to live on with enough resources for survival. The recycling of the tectonic plates keeps the density and the temperature of the planetary atmosphere and the amount of liquid water and carbon needed for life. (Hazen et al. 2002, Lineweaver 2001, Segura & Kaltenegger 2006).
2. Water: on the surface of the tectonic plates are found the oceans, formed

by H_2O . Since life on Earth is the pattern for life, water is a crucial resource for the emergence and survival of life (McClendon 1999).

3. Atmosphere: the atmosphere of a planet should be dense enough to protect the planet from UV radiation and meteoric impacts, and thin enough to allow the evolution of life on the planet's surface. The atmospheric composition of the primitive Earth allowed the origin of life and had abundance of CO , CO_2 , H_2O , N_2O , and NO_2 . Such compounds were crucial to the origin of the present atmosphere on Earth. (Bada 2004, Chyba & Sagan 1991, Maurette et al. 1995, Navarro-González et al. 2001, Sekine et al. 2003).

Since all the geophysical elements are heavier than He, the abundance of these kinds of elements necessary to create an Earth-like planet is both contained and well represented by the distribution of Z given by the chemical evolution model.

3.1.3. Biogenic characteristics

As previously mentioned, the GHZ is based on the pattern of life on Earth; therefore, in order to determine the time of the origin and development of life on Earth several studies were taken into account.

There are several theories of the means and places where life originated on Earth. Some of those theories are based on hydrothermal vents on the seabed, where an interaction between the terrestrial mantle and the ocean exists (Bada 2004, Chang 1982, Gomez-Caballero & Pantoja-Alor 2003, Hazen et al. 2002, McClendon 1999). Other theories have assumed the migration of life from other regions of space to Earth (Maurette et al. 1995, Orgel 1998). There are others explaining the catalytic effect of lightning or metallic meteorites (Chyba & Sagan 1991, Navarro-González et al. 2001, Sekine et al. 2003) in the primitive atmosphere and/or in the seas. Regardless of how life emerged, all theories have agreed on the same biogenic requirements, i.e. C, N, O, P, S. Those biogenic elements are heavier than He and the abundance of these elements is consequently contained and well represented by the distribution of Z given by the CEM.

The earliest evidence we have for life on Earth is about 3.5 Gy ago (the most ancient fossils being cyanobacteria) or 3.8 Gy (contested carbon isotope evidence). There is general agreement that life got started 3.7 Gy ago (Ricardo & Szostak 2009). The the Earth is 4.6 ± 0.1 Gy old (Bonanno et al. 2002); therefore, life took around 0.9 Gy to emerge. In consequence, in this study we consider 1.0 Gy to be the minimum age of a planet in order for basic life to appear on its surface.

On the other hand, if evolved life is associated with humans, another parameter of life should be taken into account since humans appeared on Earth 2 million years (2×10^{-3} Gy) ago (Bada 2004). However, the fact that the times used in our CE study are of the order of gigayears, this 2×10^{-3} Gy is negligible. Thus, in this study we consider 4.5 Gy to be the minimum age of a planet for complex life to evolve.

3.2. Restrictions for the GHZ

Based on the previously collected information, in order to obtain the evolution of the Galactic Habitable Zone in M31, we chose the following astronomical and biogenic restrictions:

1. Regions in the galaxy with metallicity between $-0.35 \leq \log(Z/Z_{\odot}) \leq +0.35$ are able to form most Earth-like planets.
2. Earth-like planets require 1.0 Gy to create basic life (BL).
3. Earth-like planets need 4.5 Gy to evolve complex life (CL).
4. Life on formed planets is annihilated by the supernova explosions under the following conditions:
 - (a) The SN rate at any time has been higher than the average SN rate in the solar neighborhood ($\langle RSN_{SV} \rangle$) during the last 4.5 Gy of the Milky Way's life, and
 - (b) The average RSN , during the whole existence of the planet, is higher than $\langle RSN_{SV} \rangle$

Based on: i) Planet formation, dependent on Z , is the crucial factor of the GHZ (Suthar & McKay 2012) and ii) the entire galactic disk has undergone considerable star formation, where and when the Z values are suitable for planetary formation (see Figures 4a, 4b, and 5), then the probability, $P(r, t)$, to form Earth-like planets which survive SN explosions and where basic and complex life may surge is calculated as

$$P(r, t) = P_Z(r, t) \times P_{BL}(t) \times P_{CL}(t) \times P_{SN}(r, t), \text{ where}$$

1. $P_Z(r, t)$ is the Z -dependent probability of forming terrestrial planets. We adopt a Z dependence for $P_Z(r, t)$ identical to the Z distribution shown by extrasolar planets (see Figure 5).
2. $P_{BL}(t)$ and $P_{CL}(t)$ are the probabilities of the emergence of basic life and the evolution of complex life. We adopt functions with no dispersion (equal to 0.0 or 1.0) because the uncertainties in the evidence for life are similar to the temporal resolution of the chemical evolution model.
3. $P_{SN}(r, t)$ is the probability of survival of supernova explosions. We adopt $P_{SN}(r, t) = 1.0$ or $P_{SN}(r, t) = 0.0$ if SN rate is lower or higher than the average RSN , respectively. This is a good approximation because of the quick decay of P_{SN} (Lineweaver et al. 2004) and the two extreme conditions supported on the pattern of life and considered in this study.

3.3. Results of the Galactic Habitable Zone

Our chemical evolution model—explained in section 2—provided the evolution of metals and the SN rate at different galactocentric distances, which are the data required to compute the Galactic Habitable Zone. We then applied the restrictions listed in the previous sections on the galactic disk of M31 and obtained the GHZ. Since most previous studies of the GHZ have focused on the Milky Way (Lineweaver et al. 2004, Prantzos 2008, Gowanlock et al. 2011), we also obtained the GHZ of the Andromeda galaxy using their common restrictions in order to compare the GHZ in both neighboring spiral galaxies using identical galactic habitable conditions.

3.3.1. Present work conditions

Based on the results of the chemical evolution model, we found the times and regions in the galactic disk where the metallicity condition is satisfied; we then applied the condition of supernova survival, and imposed the restriction of basic life (1 Gy) and evolved life (4.5 Gy). In Figure 6 we show the evolution of the GHZ assuming these constraints and we mark with different symbols the zone where there are enough metals to form planets (green area), where planets were sterilized (red), where planets may have basic life (striped pattern), and where planets might harbor complex life (cross-hatch pattern). We indicate with differently shaded levels the probability values of forming Earth-like planets. The yellow and blue areas represent the zones with probabilities lower than 4%, because the metallicity is too high and too low, respectively. Terrestrial planets could hardly be formed in these zones.

The only difference between the models shown in Figure 6a and Figure 6b is the assumption about planet survival with respect to the occurrence of SNe. In Figure 6a we assumed that life survives if $RSN(t)$ is smaller than $< RSN_{SV} >$ at each instant of the planet's existence. This implies that life on the planet would not recover after a nearby SN (~ 6 supernovae per million year). In Figure 6b, we considered life to survive if the average SN rate during the entire existence of the planet is lower than $< RSN_{SV} >$. This implies that life might recover or reappear after a nearby SN explosion.

The GHZs shown in Figure 6 are smaller at high planet ages (equivalent to low evolutionary time) and excludes short galactocentric radii, due to the inside-out formation scenario, upon which the chemical evolution model was built. That model predicts a high star formation rate at inner radii during the first moments of evolution and, consequently, a high SN rate that would have sterilized the planets formed there. If life has not recovered after $RSN(t) = < RSN_{SV} >$, then there can be no planets with complex life at $r < 13$ kpc (see Figure 6a), but if life does recover, there could be some planets with complex life at any r (see Figure 6b).

Based on both figures, the GHZ of M31 is located in the galactic disk and consists of a ring that widens from the central to the outer parts, from the first Gy to 5 Gy with a low probability of forming terrestrial planets. During the

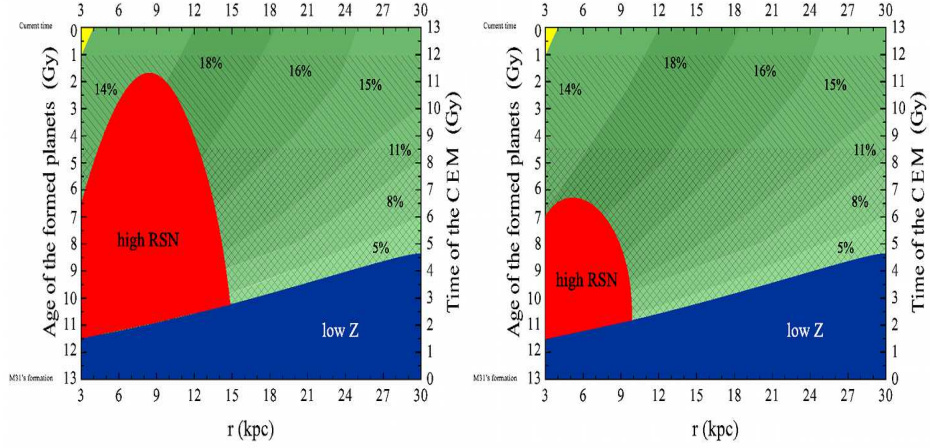


Fig. 6. Evolution of the Galactic Habitable Zone of M31 assuming our considerations (see section 3.2). Green area: zone with sufficient metallicity to form planets according to the Z distribution shown by detected stars with extrasolar planets. The width at half maximum of this distribution is located at $-0.35 \leq \log(Z/Z_{\odot}) \leq +0.35$ and the peak is at $\log(Z/Z_{\odot}) \sim 0.2$. Shaded areas: probability values of forming Earth-like planets. Yellow and blue areas: zones with probabilities lower than 4% due to the metallicity being too high and too low, respectively. In these zones terrestrial planets have hardly formed. Striped pattern: zone where planets may harbor basic life. Cross-hatched pattern: zone where planets may harbor evolved life. Red area: zone where life may be extinguished by SN explosions, comparing two different regimes of SN rate to the time-average SN rate of the solar neighborhood during the Sun's existence, $\langle RSN_{SV} \rangle$: Left: if planet sterilization occurs when the instantaneous SN rate is higher than $\langle RSN_{SV} \rangle$. Right: if planet sterilization occurs when the average SN rate during the planet's entire existence is higher than $\langle RSN_{SV} \rangle$.

next ~ 2 Gy, the ring expands into the inner parts, reaching practically the whole galactic disk, between 3 and 30 kpc, increasing the probability towards smaller radii. After 7 Gy, the high probability shifts to central radii.

The ring contains planets not older than 11 Gy, those planets with ages higher than 1 Gy harbor basic life, but evolved life might be found on planets older than 4.5 Gy. If life is annihilated with an instantaneous SN rate higher than what the Earth has experienced, most planets formed between 3 and 13 kpc and older than 2 Gy would have been sterilized, and most the probable GHZ with complex life would be located between 13 and 24 kpc. If life is extinguished with an average SN rate over the entire existence of the planet higher than that undergone by the Earth, planets formed between 3 and 10 kpc and older than 6.5 Gy would be sterilized, and the most probable GHZ with complex life would be located between 3 and 13 kpc. In either case, the halo component (for evolution times lower than 1 Gy at any r) is discarded from the GHZ because of its low Z .

3.3.2. Milky Way conditions

Four of the five previous studies of the GHZ (Gonzalez et al. 2001, Lineweaver et al. 2004, Prantzos 2008, Gowanlock et al. 2011, Suthar & McKay 2012) have focused on the Milky Way. The Milky Way is a smaller spiral galaxy than the Andromeda galaxy, with a lower halo metallicity, a steeper slope, and a lower y-intercept value of the O/H gradient; hence, the MW has had a chemical history different from that of M31. The comparison between the GHZs of the MW and M31, from the same astrophysical, geophysical and biogenic restrictions, have allowed us to explore the effect on the GHZ of the intrinsic differences among spiral galaxies. These differences are mainly the infall and the star formation history, which determine the gas enrichment in each galaxy.

Lineweaver et al. (2004), Prantzos (2008) and Gowanlock et al. (2011) have computed the GHZ of the MW assuming specific Z ranges to form Earth-like planets and for SN survival. Since Gowanlock et al. (2011) adopted a much wider Z range than that of Lineweaver et al. (2004) and with probabilities lower than that considered by Prantzos (2008), we computed the GHZ of M31 based on the assumptions of Lineweaver et al. (2004) and Prantzos (2008), separately.

First, we computed the GHZ of M31 using Lineweaver et al.'s assumptions:

i) Earth-like planets, that survive the migration of Jupiter-like planets, formed in regions where $-0.35 \leq \log(Z/Z_{\odot}) \leq +0.35$, a range that represents the width at half maximum of the distribution considered by Lineweaver et al. and peaks at $\log(Z/Z_{\odot}) \sim 0.1$. This Z distribution is poorly populated at high metallicities, according to extrasolar planets data up till 2004.

ii) Those planets formed are sterilized by the SN explosions if the time-average of the neighboring SN rate during the first 4.5 Gy of the planet's age, $\langle RSN(r, t) \rangle$, is higher than twice that of the mean SN rate in the solar neighborhood during the Earth's existence, $\langle RSN_{SV} \rangle$. Specifically, $P_{SN}(r, t) = 1.0$ or $P_{SN}(r, t) = 0.0$ if the average SN rate, during the first 4.0 Gy of the planet's existence, is lower or higher than $2 \times \langle RSN_{SV} \rangle$.

In Figure 7a we show the M31 GHZ, taking into account the previous conditions, and also we impose our basic and complex life conditions. This GHZ is similar, but not equal, to that computed with our conditions (see Figures 6) because its Z range is identical to ours, but its probability of forming Earth-like planets and its survival condition are slightly different. The central area of the galactic disk, discarded by planet sterilization, is wider than that in Figure 6b, because its survival condition (average in the first 4.0 Gy) implies that life is less resistant to SN explosions than our survival condition (averaged over the planet's entire existence). That fact, together with the low probability of forming planets at high Z , places the most probable GHZ with complex life between 10 and 19 kpc.

In Figure 7b we show the M31 GHZ taking into account the Z and survival assumptions by Prantzos (2008) plus our basic and complex life conditions. The only difference with the Lineweaver et al. conditions is the Z distribution

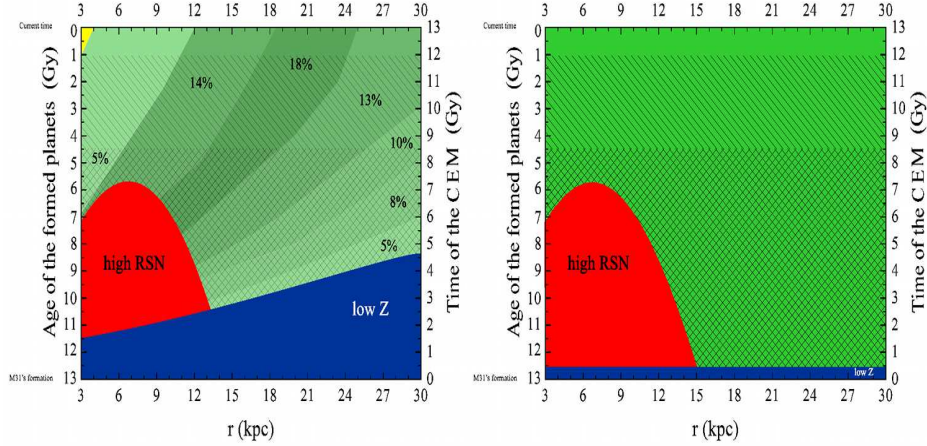


Fig. 7. Evolution of the Galactic Habitable Zone of M31 assuming the GHZ considerations for the MW (see section 3.3.2). Green area: zone with sufficient metallicity to form Earth-like planets that survive to migration of Jupiter-like planets. Shaded areas: probability values of forming those planets. Yellow and blue areas, and striped and cross-hatched patterns as in Figure 6. Red area: zone where life may be extinguished if the average SN occurrence, during the first 4.0 Gy of the planet existence, is higher than $2 \times \langle RSN_{SV} \rangle$. Left: Lineweaver et al. (2004) Z -distribution condition: $-0.35 \leq \log(Z/Z_{\odot}) \leq +0.35$ with a maximum at $\log(Z/Z_{\odot}) = +0.10$. Right: Prantzos (2008) Z -distribution: $-1.00 \leq \log(Z/Z_{\odot}) \leq +0.50$ with equal probability for each Z .

and range to form Earth-like planets that survive to the migration of Jupiter-like planets. Prantzos assumed a wider range in Z , $-1.00 \leq \log(Z/Z_{\odot}) \leq +0.50$, with an almost constant probability for any Z . Consequently, the habitable galactic zone includes the entire galactic disk since the first Gy with equal probability for each radius and time. Earth-like planets contained in this zone are as old as 12.5 Gy. In this case, the GHZ extends to the innermost regions of the disk, where Z is the highest, and to the youngest halo star, where $\log(Z/Z_{\odot}) \sim -1$.

4. DISCUSSION

4.1. Chemical Evolution model

A chemical evolution model can be computed with three minimum observational constraints at the present time: total baryonic mass, gas mass, and the abundance of one chemical element. In this study we have compiled from the updated literature and well described $\Sigma_T(r)$ and $\Sigma_{gas}(r)$ distributions, and we have determined a precise O/H gradient from H II regions. Based on these quite restrictive constraints, we obtained a solid chemical evolution model of the halo and disk of M31.

The chemical evolution model was built to match the most probable O/H gradient, $[O/H](r) = -0.015 \text{ dex kpc}^{-1} \times r(\text{kpc}) + 0.44 \text{ dex}$, determined considering the intrinsic scatter and several theoretical calibrations (see section

2.1.2). This gradient is caused by the inside-out scenario: the infall is faster and more abundant in inner regions, producing a more efficient SFR, which increases the O/H abundance of the inner parts faster than that of the outer parts.

In this study, we also explored the gradient determined by empirical calibrations and proposed by Pilyugin (2001) and Pilyugin & Thuan (2005). The gradient obtained through the Pilyugin (2001) calibration presents the same slope, but its y-intercept value is lower by 0.42 dex than that obtained from theoretical calibrations. On the other hand, the gradient obtained by using the Pilyugin & Thuan (2005) calibration, $[O/H](r) = -0.008 \text{ dex kpc}^{-1} \times r(\text{kpc}) - 0.23 \text{ dex}$, is $0.007 \text{ dex kpc}^{-1}$ flatter and the y-intercept value lower by 0.67 dex than that obtained from theoretical calibrations. We were not able to reproduce the Pilyugin gradient without overestimating the $\Sigma_{gas}(r)$ distribution.

Peimbert et al. (2007) suggested that the abundances derived from the R_{23} empirical calibrations could be underestimated due to the presence of temperature variations in the ionized volume, which leads to the overestimation of the electron temperatures, and that the use of empirical calibrations based on optical recombination line measurements (which are much less affected by temperature variations and give abundances similar to those obtained using theoretical calibrations) could reconcile the R_{23} theoretical calibrations with empirical ones. This is a well known problem in the astrophysics of photoionized nebulae (see Peimbert et al. 2007 and references therein for more discussion about this topic).

The slope of the O/H gradients which we computed are in some way steeper, but are consistent, within the errors, to those derived from supergiants within 12 kpc of the galactic center reported by Trundle et al. (2002), which amounts to $-0.006 \pm 0.020 \text{ dex kpc}^{-1}$. Venn et al. (2000) had also found that there was no oxygen gradient between 10 kpc and 20 kpc; however, their study was based on abundance determinations for only three A–F supergiants and their results are therefore inconclusive. Kwitter et al. (2012) have recently computed a radial [O/H] gradient from planetary nebulae (PNe) data. They determined a gradient of $-0.011 \pm 0.004 \text{ dex kpc}^{-1}$, which is consistent to within the errors with our value derived from H II regions.

We need additionally to bear in mind that, although the values of the gradient we have obtained are somewhat shallower than typical values for spiral galaxies, recent results seem to confirm that M31 is a barred spiral galaxy (see Beaton et al. 2007, Athanassoula & Beaton 2006 and references therein), which produce shallower gradients than normal spiral galaxies (Friedli et al. 1994).

The Σ_{gas} obtained from the chemical evolution model follows a similar pattern to that observed at radii larger than 9 kpc. However, at smaller radii the model predicted more gas than observed. Since Σ_{gas} , at a fixed galactocentric distance, decreases due to the SFR and increases mainly due to infall, we tried to reproduce at smaller r values the Σ_{gas} increasing the SFR,

but the slope of the O/H gradient became steeper than the most probable one. In addition, we tried to solve the discrepancy between the model and the observed Σ_{gas} at low radii, changing the radial distribution of the infall, but the agreement with the observed Σ_T was lost. It is possible to reduce Σ_{gas} in the inner part by adopting gas inflows to the galactic bar (Portinari & Chiosi 2000, Spitoni & Matteucci 2011). That assumption will be considered in a future article.

The predicted distribution of the SFR at 13 Gy agrees with the observed one (see data collected by Yin et al. 2009 and Marcon-Uchida et al. 2010) for inner regions, but is in disagreement for outer regions. On the other hand, the agreement between the predicted and observed Σ_{gas} is good for the outer regions, but not for inner regions. Since the SFR assumed in this study depends on the gas mass, there is an inconsistency between the observed Σ_{gas} and the SFR. Therefore, it is not obvious how to change the two free parameters of our SFR (see section 2.2) to match both the Σ_{gas} and the SFR distributions with the observed values. In order to improve the agreement of the obtained Σ_{gas} and SFR, we needed to consider different accretion and star formation laws based on more complex physical properties for galactic and star formation.

Renda et al. (2005), Matsson (2008), Yin et al. (2009), and Marcon-Uchida et al. (2010) have computed CEMs for the Andromeda galaxy taking into consideration different assumptions and using diverse codes. These models were built to reproduce different O/H gradients, which show higher dispersion or error, with O/H differences at a given r value in the 0.4 to 0.7 dex range; consequently, these models are not constrained as well as our model. In particular the agreements of the Marcon-Uchida et al. model are poorer or marginal.

We also made a comparative study of the chemical evolution models and the observational constraints of the Milky Way galaxy with the Andromeda galaxy, and we noticed that:

1. The maximum average of the Fe/H abundances present in the halo stars of M31 corresponds to $\log(Z/Z_{\odot}) = -0.5$, while in the MW it amounts to -1.6 (Koch et al. 2008). In order to reproduce the higher Z value in the halo stars of M31, our model requires, in the halo phase, a more efficient infall (τ_h is about 5 times lower) and SFR (two orders of magnitudes higher) than those for the MW model computed with similar assumptions (Carigi et al. 2005, Carigi & Peimbert 2011).
2. The adopted gradient for M31, $[O/H](r) = -0.015 \text{ dex kpc}^{-1} \times r \text{ (kpc)} + 0.44 \text{ dex}$, is 0.03 dex flatter and 0.06 dex higher in the central value than the O/H gradient of the Milky Way disk determined by Esteban et al. (2005) from optical oxygen recombination lines. In order to reproduce the flatter M31 gradient, our model needed, in the disk phase, a less marked inside-out formation, i.e. slower infall in the inner regions and faster accretion in the outer parts compared to the infall considered

in CEMs of the MW. Moreover, to reach the higher O/H values, the model required a more active star formation history than that assumed for the MW disk (Carigi & Peimbert 2011), resulting in a lower $\Sigma_{gas}(r)$ in M31 than in the MW, in agreement with the observed distribution in both galaxies.

4.2. Galactic Habitable Zone

The chemical evolution model discussed above provides the evolution and location of the heavy elements of which planets are formed and the rate of neighboring SNe that may sterilize life on the planets. The age and the location of Earth-like planets inside a galaxy depend mainly on the Z range assumed to form those planets.

It is difficult to quantify the role of metallicity in planet formation. At present, theoretical models fail to explain in detail the physical processes in protoplanetary disks and in particular the metallicity effect on the planet mass (rocky like Earth or gaseous like Jupiter). Furthermore, the observational data of detected extrasolar planets do not show a clear trend between the stellar metallicity and the planet mass that orbit around it. Recent studies (e.g. Jenkins et al. 2012) have increased the dispersion in the stellar Z –planet mass relation to detect more low-mass planets around metal-rich stars. Also, it is noticeable that in many detected extrasolar planetary systems, Earth-like and Jupiter-like planets coexist (The Extrasolar Planets Encyclopedia). Moreover, Raymond et al. (2006) have simulated terrestrial planet growth during and after giant planet migration. Observational studies on the circumstellar disk in young stellar clusters of low and solar metallicities suggest that the disk lifetime shortens with decreasing Z , thereby reducing the time available for planet formation (Yasui et al. 2010). Based on circumstellar disk models and dust grain properties, Johnson & Li (2012) conclude that the first Earth-like planets likely formed from gas with metallicities $Z > 0.1 Z_{\odot}$.

For these reasons we adopted the Z distribution shown by planet-harboring stars as the metallicity condition for the GHZ instead of undertaking a probability study of planet formation and migration as a function of metallicity, as did Lineweaver (2001), Prantzos (2008), and Gowanlock et al. (2011). Using that Z distribution, the GHZ currently extends in the galactic disk from 3 to 30 kpc with maximum planet ages of 11 and 8.5 Gy, respectively. The most probable GHZ, considering only basic life, is between 6 and 17 kpc and ages between 1 and 4.5 Gy; assuming complex life, however, the most probable GHZ is between 3 and 13 kpc and ages between 4.5 and 6.5 Gy (see Figure 6b). When we adopted the Z distribution by Lineweaver, with a lower number of exoplanets at high metallicities, the most probable GHZ, considering only basic life, is between 13 and 24 kpc and ages between 1 and 4.5 Gy, but, assuming complex life, the most probable GHZ is between 10 and 19 kpc and ages between 4.5 and 8 Gy (see Figure 7a). In both cases, the formation of Earth-like planets was discarded in the Andromeda halo

since that galactic component contributes with very low amounts of metals ($\log(Z_{halo}/Z_{\odot}) < -0.5$, see Figure 4a).

When we adopted the Z condition by Prantzos, ($-1.00 \leq \log(Z/Z_{\odot}) \leq +0.50$), the first planets formed are older than the galactic disk and a few Earth-like planets might even be formed in the halo because the maximum Z shown by the halo stellar population is 0.5 dex higher than the minimum Z required ($\log(Z/Z_{\odot}) = -1.00$) to form Earth-like planets. It is important to remark that only in this case have Earth-like planets surviving Jupiter-like ones been formed in the innermost regions, because the maximum metallicity reached by the model is $\log(Z/Z_{\odot}) = +0.4$ (see Figure 7b).

The age and the location of Earth-like planets sterilized by SN explosion inside a galaxy is determined by the assumed SN condition. That condition is the most uncertain restriction, because it is difficult to estimate the resistance of life to SN explosions, which depends on unknown biogenic and astrophysical factors, such as the minimum SN-planet distance that allows life to survive, the type of atmosphere and oceans where life could evolve, and the biological properties of the different types of life, among others factors.

Since our life pattern is based on one Earth, life that has been able to recover from neighbor SN events, and the solar neighborhood has undergone a nearby constant and low SN rate from its formation (Renda et al. 2005, Prantzos 2008, Carigi & Peimbert 2008), we have assumed that the average SN rate of the solar neighborhood is the maximum one that life can withstand during the whole planet evolution. Using that SN restriction, planets older than 6.5 Gy and located at $r < 10$ kpc were sterilized (see Figure 6b). When we assumed the SN condition by Lineweaver et al. (2004), a less restrictive constraint that considers the time-average of the SN rate during the first 4.0 Gy life of the planet, only planets older than 6 Gy located at $r < 13$ kpc have been sterilized (see Figure 7a). In all cases, even though the area subtracted from the GHZ due to SN explosion is small, the number of planets where life has disappeared is significant because the stellar mass decreases with the galactocentric radius, following an exponential behavior given by the luminosity profile (see section 2.1.1).

In a future paper, the $SFR(r,t)$ will be considered to compute the GHZ as the most likely zone to have stars with habitable planets. In that case, the GHZ will be located even further towards the centre of the disk of M31, similarly to the GHZ of MW obtained by Prantzos (2008) and Gowanlock et al. (2012). Since the stellar mass profile of M31 is flatter than that of the MW, it will be interesting to know how wide the M31 GHZ is and to quantify the number of planet-harboring stars.

Using the same astrophysical, geophysical, and biogenic restrictions in M31 as those considered in the MW studies (Lineweaver et al. 2004, Prantzos 2008), we found that the GHZ of M31 is wider compared to that of the MW. This result is mainly due to the higher and flatter Z gradient of the disk of M31. Consequently, the outer parts of the disk are more metal-rich and able to form planets. In addition, we found that the GHZ of M31 is older due to

the higher metallicity of the halo, causing the first stellar generations of the disk to have more heavy elements to form planets than the first stars of the MW (See Figures 6).

Throughout this section we have emphasized that the chemical content is the most restrictive condition to the GHZ. Furthermore, we have mentioned that the slope of the Z gradient is determined by the efficiency of inside-out scenario, whereas the y-intercept values of the gradient depend on by the amount of accreted gas and the star formation efficiency. Therefore, we stress that the manner in which a galaxy is assembled and its stars formed determine the size and age of the Galactic Habitable Zone.

5. CONCLUSIONS

Based on O/H values of H II regions, we obtained O/H gradients with different empirical and theoretical calibrations. In the presence of intrinsic scatter, we computed the most probable gradient for M31 from theoretical calibrations based on the R_{23} method and we found that $[O/H](r) = -0.015 \pm 0.003 \text{ dex kpc}^{-1} \times r(\text{kpc}) + 0.44 \pm 0.04 \text{ dex}$. The slope of the gradient is $0.03 \text{ dex kpc}^{-1}$ flatter, and the value at the center of the galaxy is 0.06 dex higher, than those values of the O/H gradient of the Milky Way disk.

The chemical evolution model built to reproduce our precise O/H gradient of the galactic disk matches the radial distribution of the gas mass, $\Sigma_{gas}(r)$, for the outer regions quite well, but it fails for the inner ones. On the other hand, the radial distribution of the star formation rate, $SFR(r)$, fits for the inner parts, but not for the outer ones. Therefore, in order to improve the agreements, the model would require more complex galactic and star formation histories.

The model cannot reproduce the O/H gradient computed by empirical methods, which is 0.42 dex lower for the central value than the gradient obtained by theoretical methods, unless the other observational constraints are considerably modified.

Based on the chemical evolution model we obtained, for the first time, the Galactic Habitable Zone (GHZ) of M31, considering two space requirements: regions with i) sufficient metallicity for planet formation with a probability law that follows the Z distribution shown by exoplanets and ii) an average SN rate similar to that permitting the existence of life on the Earth; and two time requirements: the existence of basic life (like cyanobacteria), and the development of evolved life (like humans).

The GHZ of M31 is located in the galactic disk and consists of a ring that widens from the inner to the outer parts, during the last $\sim 11 \text{ Gy}$ of evolution, reaching at the present time practically the whole galactic disk. If life is extinguished with an average SN rate higher than that for the Earth during the planet's entire existence, planets formed between 3 and 10 kpc and older than 6.5 Gy would have been sterilized. If only basic life is considered, the most probable GHZ corresponds to 28% of the galactic disk area and this GHZ is located between 6 and 17 kpc on planets with ages between 4.5 and 1

Gy. If complex life is considered, the most probable GHZ corresponds to 18% of the galactic disk area and is located between 3 and 13 kpc on planets with ages between 6.5 and 4.5 Gy.

In GHZ studies, the Z restriction is crucial for finding the location of Earth-like planets, but the SN survival condition allows us to compute the location of those planets that survive SN events.

Since M31 is more metal-rich than the MW (specifically the metallicity of the halo is higher and the chemical gradient of the galactic disk is flatter and higher compared to the Galaxy), the GHZ of M31 is wider and older than that of the MW. Therefore, the number of planets harboring life in Andromeda could be higher than in our galaxy.

Part of this work was submitted by Sofía Meneses Goytia to the Master's Programme in Sciences Chemistry at the Universidad Nacional Autónoma de México.

6. ACKNOWLEDGMENTS

The authors thank C. Esteban for his timely suggestion concerning the O/H gradient; they also thank M. Peimbert, A. Segura for a critical reading of the manuscript and T. Mahoney for revising the english text. L. Carigi thanks E. M. Berkhuijsen for kindly providing information about gas data of M31 and detailed explanations of how to compute the hydrogen gas mass. S. Meneses-Goytia thanks T.J.L. de Boer and S. C. Trager for their careful and detailed review of the present paper. J. García-Rojas acknowledges partial support from the project AYA2007-63030 of the Spanish Ministerio de Educación y Ciencia and from a UNAM postdoctoral grant. L. Carigi thanks the funding provided by the Ministry of Science and Innovation of the Kingdom of Spain (grants AYA2010-16717 and AYA2011-22614). This work was partly supported by grant 129753 from CONACyT.

REFERENCES

- Akritas, M. G., & Bershadsky M. A. 1996, *ApJ*, 470, 706
- Athanassoula, E., & Beaton, R. L. 2006, *MNRAS*, 370, 1499
- Bada, J. L. 2004, *Earth & Planetary Science Letters*, 226, 1
- Barnes, R., Raymond, S. N., Jackson, B., & Greenberg, R. 2008, *Astrobiology*, 8, 557
- Beaton, R. L., Majewski, S. R., Guhathakurta, P., Skrutskie, M. F., Cutri, R. M., Good, J., Patterson, R. J., Athanassoula, E., & Bureau, M. 2007, *ApJL*, 658, L91
- Blair, W. P., Kirshner, R. P., & Chevalier, R. A. 1982, *ApJ*, 254, 50
- Bonanno, A., Schlattl, H., & Paternù, L. 2002, *A&A*, 390, 1115
- Carigi, L., Peimbert, M., Esteban, C., García-Rojas, J. 2005, *ApJ*, 623, 213
- Carigi, L., Peimbert, M. 2008, *RevMexAA* 44, 341
- Carigi, L., Peimbert, M. 2011, *RevMexAA*, 47, 139
- Chang, S. 1982, *Physics of the Earth & Planetary Interiors*, 29, 261

- Chyba, C., & Sagan, C. 1991, *Origins Life & Evolution of the Biosphere*, 21, 3
- Fogg, M. J., & Nelson, R. P. 2007, *A&A*, 472, 1003
- Franco, I., & Carigi, L. 2008, *RevMexAA*, 44, 311
- Friedli, D., Benz, W., & Kennicutt, R. 1994, *ApJL*, 430, L105
- Fuchs, B., Jahreiβ, H., & Flynn, C. 2009, *AJ*, 137, 266
- Galarza, V. C., Walterbos, R. A. M., & Braun, R. 1999, *AJ*, 118, 2775
- Gómez-Caballero, J. A., & Pantoja-Alor, J. 2003, *Boletín de la Sociedad Geológica Mexicana*, LVI, 56
- Gonzalez, G., Brownlee, D., & Ward, P. 2001, *Icarus*, 152, 185
- Gowanlock, M. G., Patton, D. R., & McConnell, S. M. 2011, *Astrobiology*, 11, 855
- Grevesse, N., Asplund, M., & Sauval, A. J. 2007, *Space Science Reviews*, 130, 105
- Hazen, R. M., Boctor, N., Brandes, J., Cody, G. D., Hemley, R. J., Sharma, A., & Yoder, H. S. 2002, *Journal of Physics, Condense Matter*, 14, 11489
- Holland, S. 1998, Ph. D. thesis from the University of British Columbia, Canada.
- Horner, J., & Jones, B. W. 2008, *International Journal of Astrobiology*, 7, 251
- Horner, J., & Jones, B. W. 2009, *International Journal of Astrobiology*, 8, 75
- Hughes, G. L., Gibson, B. K., Carigi, L., Sánchez-Vázquez, P., Chavez, J. M., & Lambert, D. L. 2008, *MNRAS*, 390, 1710
- Jenkins et al. 2012, *ApJ* submitted (arXiv:1207.1012)
- Jiménez-Torres, J. J., Pichardo, B., Lake, G., & Throop, H. 2011, *MNRAS*, 418, 1272
- Johnson, J. L. & Li, H. 2012, *ApJ*, 751, 81
- Kennicutt A. 1998, *ApJ*, 498, 541
- Kewley, L. J., & Dopita, M. A. 2002, *ApJS*, 142, 35
- Koch, A., Rich, R. M., Reitzel, D. B., Martin, N. F., Ibata, R. A., Chapman, S. C., Majewski, S. R., Mori, M., Loh, Y. S., Ostheimer, J. C., & Tanaka, M. 2008, *ApJ*, 689, 958
- Kobulnicky, H. A., & Kewley, L. J. 2004, *ApJ*, 617, 240
- Kroupa, P., Tout, C. A., & Gilmore, G. 1993, *MNRAS*, 262, 545
- Kwitter, K. B., Lehman, E. M. M., Balick, B., & Henry, R. B. C. 2012, *ApJ*, 753, 12
- Lineweaver, C. H. 2001, *Icarus*, 151, 307
- Lineweaver, C. H., Fenner, Y., & Gibson, B. K. 2004, *Science*, 303, 59
- Marcon-Uchida, M. M., Matteucci, F., & Costa, R. D. D. 2010, *A&A*, 520, 35
- Mattsson, L. 2008, *Physica Scripta*, 133, 014027
- Maurette, M., Brack, A., Kurat, G., Perreau, M., & Engrand, C. 1995, *Advances on Space Research*, 15, 113
- Meneses-Goytia, S. 2009, Master in Sciences Chemistry, Universidad Nacional Autónoma de México.
- McClendon, J. H. 1999, *Earth-Science Reviews*, 47, 71
- McGaugh, S. S. 1991, *ApJ*, 380, 140
- Navarro-González, R., McKay, C. P., & Nna-Mvondo, D. 2001, *Nature*, 412, 61
- Nieten, Ch., Neininger, N., Guélin, M., Ungerechts, H., Lucas, R., Berkhuijsen, E. M., Beck, R., & Wielebinski, R. 2006, *A&A*, 453, 459
- Orgel, L. E. 1998, *Trends in Biochemical Sciences*, 23, 491
- Pagel, B. E. J., Edmunds, M. G., Blackwell, D. E., Chun, M. S., & Smith, G. 1979, *MNRAS*, 189, 95
- Peimbert, M., Peimbert, A., Esteban, C., García-Rojas, J., Bresolin, F., Carigi, L., Ruiz, M. T., & López-Sánchez, A. R. 2007, *RevMexAASC*, 29, 72

- Pilyugin, L. S. 2001, *A&A*, 373, 56
- Pilyugin, L. S., & Thuan, T. X. 2005, *ApJ*, 631, 231
- Prantzos, N. 2008, *Space Science Reviews*, 135, 313
- Portinari, L. & Chiosi, C. 2000, *A&A*, 355, 929.
- Raymond, S. N., Mandell, A. M., & Sigurdsson, S. 2006, *Science*, 313, 1413
- Renda, A., Kawata, D., Fenner, Y., & Gibson, B. K. 2005, *MNRAS*, 356, 1071
- Ricardo, A. & Szostak, J. W. *SciAm*, September 2009, p. 250
- Rosolowsky, E., & Simon, J. D. 2008, *ApJ*, 675, 1213
- Sarajedini, A., & Jablonka, P. 2005, *AJ*, 130, 1627
- Segura, A., & Kaltenegger, L. 2009, *Emergence, Search & Detection of Life*. Edited by V. A. Basiuk, American Scientific Publishers, 1
- Sekine, Y., Sugita, S., Kadono, T., & Matsui, T. 2003, *Journal of Geophysical Research*, 108,
- Sleep, N. H., Bird, D. K., Pope, E. 2012, *Annual Review of Earth and Planetary Sciences*, 40, 277
- Spitoni, & Matteucci, F. 2011 *A&A*, 531, 72
- Suthar, F. & McKay, C. P. 2012, *International Journal of Astrobiology*, 11, 157
- Trundle, C., Dufton, P. L., Lennon, D. J., Smartt, S. J., & Urbaneja, M. A. 2002, *A&A*, 395, 519
- Venn, K. A., McCarthy, J. K., Lennon, D. J., Przybilla, N., Kudritzki, R. P., & Lemke, M. 2000, *ApJ*, 541, 610
- Ward, P. D., & Brownlee, D. 2000, *Book Review - Rare earth, why complex life is uncommon in the universe? Copernicus/Springer 2000, Icarus*, 147, 325
- Widrow, L. M., Perrett, K. M., & Suyu, S. H. 2003, *ApJ*, 588, 311
- Yasui, C., Kobayashi, N., Tokunaga, A. T., Saito, M., & Tokoku, C. 2010, *ApJL*, 723, L113
- Yin, J., Hou, L. K., Prantzos, T. A., Boissier, S., Chang, R. X., Shen, S. Y., & Zhang, B. 2009, *A&A*, 505, 497
- Zaritsky, D., Kennicutt, R. C., & Huchra, J. P. 1994, *ApJ*, 420, 87

Leticia Carigi: Instituto de Astronomía, Universidad Nacional Autónoma de México. Apartado Postal 70-264, Ciudad Universitaria, México DF 04510, México (carigi@astro.unam.mx).

Sofia Meneses-Goytia: Kapteyn Instituut, Rijkuniversiteit Groningen. Landleven 12, 9747 AD, Groningen, Nederland (s.meneses-goytia@astro.rug.nl).

Jorge García-Rojas: Instituto de Astrofísica de Canarias. E-38200. La Laguna, Tenerife, Spain. Departamento de Astrofísica, Universidad de La Laguna. E-38205. La Laguna, Spain (jogarcia@iac.es).